

Thrust Scaling in a Direct Wave-Drive Thruster

Matthew S. Feldman* and Edgar Y. Choueiri†

Electric Propulsion and Plasma Dynamics Lab, Princeton, New Jersey, 08544, USA

The scaling of antenna-plasma momentum coupling in a Direct Wave-Drive Thruster (DWDT) was investigated analytically and experimentally in order to clarify the general thrust scaling in such an accelerator. The analytical model extends previous work by including the full dispersion relationship and predicts that thrust improves with increasing excitation frequency. Experimental validation was indirectly carried out using a Mach probe to measure the plasma velocity in the plume of the DWDT Experiment. The plume Mach number was measured for a constant configuration of the plasma source density and background magnetic field while varying the current and frequency of the accelerating antenna. The change in Mach number was observed to be consistent with our model's scaling predictions.

Nomenclature

T	Thrust or Momentum transfer
J	rms Current
ω, f	Frequency (rad/s, Hz)
M	Mach number
$I_{u,d}$	Ion saturation currents
H	Lengthscale of the wave-launching antenna
k	Wavenumber
c_s	Sound speed
v_f	Plume flow velocity
v_A	Alfvén velocity
ω_{pi}	Ion plasma frequency

I. Introduction

The Direct Wave-Drive Thruster (DWDT) is a new propulsion concept that uses waves to transfer momentum directly to a plasma.¹⁻⁴ As an inherently electrodeless device, a DWDT can avoid lifetime limitations due to erosion, as well as utilize a variety of propellants. Previous waves-based thruster concepts have used a variety of waves to heat a plasma and obtain thrust by expanding through a magnetic nozzle.⁵⁻⁷ In contrast, a DWDT attempts to couple directed wave momentum into a plasma for acceleration. Theoretically, this momentum transfer can be achieved inductively in a similar manner to Pulsed Inductive Thrusters (PIT).^{8,9} The key difference is a DWDT operates continuously to inject wave momentum, whereas PIT discharges its energy in a single pulse.

Previous work on the DWDT focused on the force coupling between the antenna and plasma for various wave modes of interests. More recently, we observed a tail of higher energy ions in the plume of the Direct Wave-Drive Thruster Experiment (DWDTX)⁴ using a retarding potential analyzer (RPA). This tail was only observed for lower background magnetic fields, but suggests experimentally that there is a region of interest for observing plasma acceleration in this system. However, because the RPA naturally generates a

*Ph.D. Candidate; Mechanical and Aerospace Engineering, Princeton University, Research Assistant.

†Chief Scientist, EPPDyL; Mechanical and Aerospace Engineering, Princeton University; Professor, Applied Physics Group; AIAA Fellow

significant spread in the measured ion energies and the DWDTX is not optimized for high performance, the RPA measurements are difficult to use to corroborate the scaling behavior of the system.

Based on previous analyses, we expect to see increased coupling to the plasma, and consequently increased plasma acceleration, for higher applied frequencies when targeting the magnetosonic mode.³ However, the scaling of thrust with frequency has not previously been derived for the operating regime of the DWDTX. In this paper, we extend our previous analytical thrust model to include the full dispersion relationship. We then approximate the thrust in the regime of interest to determine the scaling of thrust with respect to frequency.

In order to validate the thrust scaling behavior, we use a Mach probe to measure the increase in the plume Mach number, ΔM , as current and frequency are increased. However, ΔM is not a direct measurement of the momentum added by to the plasma. Since $T = \dot{m}v_{ex}$ and $M = v/c_s$, the increase in Mach number is only proportional to added thrust when the plume temperature and mass flow remain constant. We measure the electron temperature in the exhaust plume, and it does not change substantially with increased power to the WLA. While the mass flow of neutral argon is kept constant during our data collection, we have not yet demonstrated that \dot{m} of the plasma remains constant in the system as power is increased. Therefore, ΔM only serves as an indirect measurement of momentum added by the wave-launching antenna.

The layout of this paper will proceed as follows. In Section II, we will derive the low-frequency scaling behavior of momentum transfer in the DWDTX. In Section III, we will present the experimental set-up and describe the diagnostics and data collection process. In Section IV, we will present the plume Mach number measurements and compare their scaling with our theoretical model.

II. Thrust Model for the DWDTX

For a simplified analytical geometry, we previously determined that thrust is maximized for high frequencies.³ However, that analysis assumed an excitation frequency below the ion cyclotron frequency. In our configuration, we target a range of frequencies closer to the lower hybrid frequency and therefore must include a more complete dispersion relationship. Additionally, the previous geometry did not include a current return path, which is necessary to accurately capture the physics in our proof-of-concept experiment. In this paper, we include a current return path (shown in Figure 1) and the full cold, magnetized dispersion relationship.

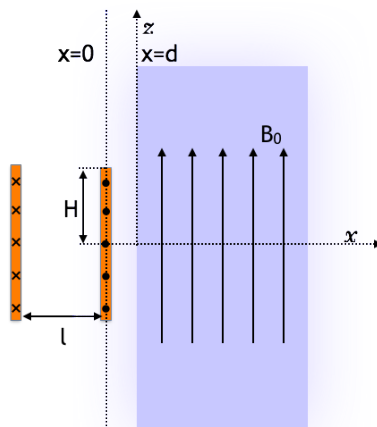


Figure 1. Analytical Geometry for Thrust Model. For the analytical model, we use the above geometry to calculate thrust. \hat{x} is the thrust direction and \hat{z} is the direction of the embedded magnetic field. The \hat{y} direction is assumed to be uniform. The WLA has a half-width of H , and the front surface of the antenna is d away from the plasma. A current return path is included a distance l away from the forward current path. This return path was not included in our previous model.³

Using the same methodology as our previous work,^{1,3} we calculate the total magnetic fields in each region

of the geometry, then calculate the total thrust by integrating the $J \times B$ force on the antenna given by:

$$T = \frac{1}{\pi} \mu_0 J_a^2 \cdot \text{Re} \left[\int_0^\infty H \left(\frac{\sin(k_z H)}{k_z H} \right)^2 (1 - e^{-k_z l})^2 (e^{-k_z d})^2 \left(\frac{k_z + ik_x}{k_z - ik_x} \right) dk_z \right], \quad (1)$$

where J_a is the rms current in the WLA, $k_{x,z}$ are the perpendicular and parallel wavenumbers, and H, l, d are the lengths shown in Figure 1. For the parameter space of the DWDTX and assuming a uniform plasma source, the dispersion relation, $k_x = k_x(\omega, k_z)$, is given by:

$$k_x^2 = \frac{\omega^2}{c^2} S - k_z^2 - \frac{\frac{\omega^4}{c^4} D^2}{\frac{\omega^2}{c^2} S - k_z^2}, \quad (2)$$

where S and D are the typical parameters derived by Stix.¹⁰

The integrand can be broken up into two components: a geometry dependent component that includes $\left(\frac{\sin(k_z H)}{k_z H}\right)^2 (1 - e^{-k_z l})^2 (e^{-k_z d})^2$, and a wave-mode dependent component given by $\bar{k}_z + i\bar{k}_x/\bar{k}_z - i\bar{k}_x$. The wave-mode component is the only frequency dependent term. To approximate the scaling behavior, we first need to limit the integration to physically relevant wave-modes. Equation 1 was derived assuming the plasma extends infinitely in the \hat{x} -direction. However, because the source plasma in our experiment has finite extent, we can only couple to wave-modes with sufficiently small wavelengths and therefore large k_x . Therefore, we limit the integration over k_z such that $k_x H > 1$. We define the maximum k_z , k_{zm} , such that:

$$\frac{1}{H^2} = \frac{\omega^2}{c^2} S - k_{zm}^2 - \frac{\frac{\omega^4}{c^4} D^2}{\frac{\omega^2}{c^2} S - k_{zm}^2}. \quad (3)$$

For the frequency range of interest in the DWDTX, between the ion cyclotron and lower hybrid frequency, we can approximate Equation 3 such that

$$k_{zm} \approx \omega \frac{H \omega_{pe}^2}{c^2 \Omega_e}. \quad (4)$$

Finally, because k_z is small and k_x is sufficiently large, we can approximate the wave-mode term as unity and Taylor expand the geometric portion of the integrand. For sufficiently high frequencies, this model requires more terms of the Taylor expansion, but for the frequencies we can reach in the DWDTX, two terms are sufficient. Therefore, we approximate the total force on the antenna as

$$T \approx \frac{1}{\pi} \mu_0 J_a^2 H \cdot \int_0^{k_{zm}} l^2 (k_z^2 - (l+d)k_z^3) dk_z, \quad (5)$$

which can be evaluated to

$$T \approx \frac{\mu_0}{3\pi} \frac{H^4 l^2 \omega_{pe}^6}{c^6 \Omega_e^3} \left(1 - \frac{3(l+d)H\omega_{pe}^2}{4c^2 \Omega_e} \omega \right) \omega^3 J_a^2. \quad (6)$$

And for convenience, we define the thrust coefficient as

$$C_T(\omega, n_e, B_0, H, l, d) = \frac{\mu_0}{3\pi} \frac{H^4 l^2 \omega_{pe}^6}{c^6 \Omega_e^3} \left(1 - \frac{3(l+d)H\omega_{pe}^2}{4c^2 \Omega_e} \omega \right) \omega^3. \quad (7)$$

The key takeaway is that the total force on the antenna increases with increasing frequency when in the parameter regime of the DWDTX.

III. Direct Wave Drive Thruster Experiment

The Direct Wave-Drive Thruster Experiment consists of a plasma source antenna (PSA), a confining magnetic field, and a wave-launching antenna (WLA). The set-up (illustrated below in Figure 2), is mounted in the EPPDyL's "Orange" Vacuum Facility. The full configuration is described in our previous work,⁴ but we will highlight the important features again here for completeness.

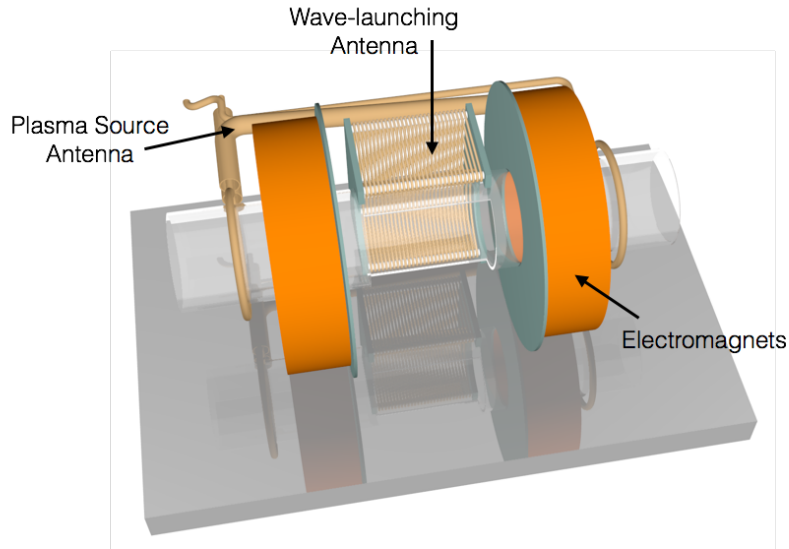


Figure 2. The Direct Wave-Drive Thruster Experiment (DWDTX). The DWDT experiment is mounted in the EPPDyL’s “Orange” Vacuum Tank. It consists of a confining glass tube with an exhaust hole centered between two electromagnets (in orange), which creates a magnetic bottle. Gas is injected from either side of the tube and a plasma is created using a 13.56 Mhz RF signal by the two copper loop antennas bracketing the electromagnets. The WLA is center mounted behind the exhaust hole. G10 plates (shown in green) isolate the electromagnets from direct exposure to the plume. Not pictured are two Macor backplates which seal the open ends of the tube, through which argon gas is injected.

A. Experimental Set-Up

The DWDTX plasma source consists of a linear magnetic bottle contained in a 8 cm diameter pyrex tube and confined by two electromagnets spaced 12 cm apart. In this paper, B_0 is defined as the magnetic field strength at the center of the magnetic bottle configuration. The pyrex tube has an 8 cm x 8 cm exhaust hole centered between the magnets. The PSA (outline in red in Figure 3) consists of a dual loop antenna which encircles each end of the glass tube. Finally, argon gas is fed through both ends of the tube, ionized by the PSA and allowed to flow along the magnetic field lines to the center of the structure and eventually out of the exhaust hole.

The WLA (outlined in blue in Figure 3) is positioned between the two field coils directly behind the exhaust hole. The antenna is designed to couple to the magnetosonic mode, such that the antenna current paths are perpendicular to the background magnetic field. The antenna is wound to contour to the outside of the tube; a single sample winding can be seen in Figure 4. While our previous antenna had 30 windings,⁴ this WLA has 36 windings, which is expected to improve overall antenna-plasma coupling.

B. Diagnostics

1. Langmuir Probe

The Langmuir Probe (LP) in our system is a 1 mm diameter, 3.5 mm length, tungsten rod mounted inside an alumina tube. The probe is powered by a bipolar operational amplifier and was swept at 3Hz from -40 to 90 V and averaged over 4 sweeps. The current was sensed over a 1000 Ω resistor and low pass filter. The filter removes RF noise and has a 3dB cut off of 25 kHz. The electron temperature is obtained as usual from the slope of the $\ln(I_e) - V$ trace.¹¹

2. Mach Probe

Mach probes (MP) are electrostatic probes that measure the flow Mach number, $M = v_f/c_s$, where v_f is the flow velocity and c_s is the sound speed.¹² The basic design includes two probe tips separated by an insulator and biased into the ion saturation regime. For a stationary plasma, each probe tip will draw equal ion saturation currents. However, if plasma is flowing perpendicularly to the collection surfaces (as shown

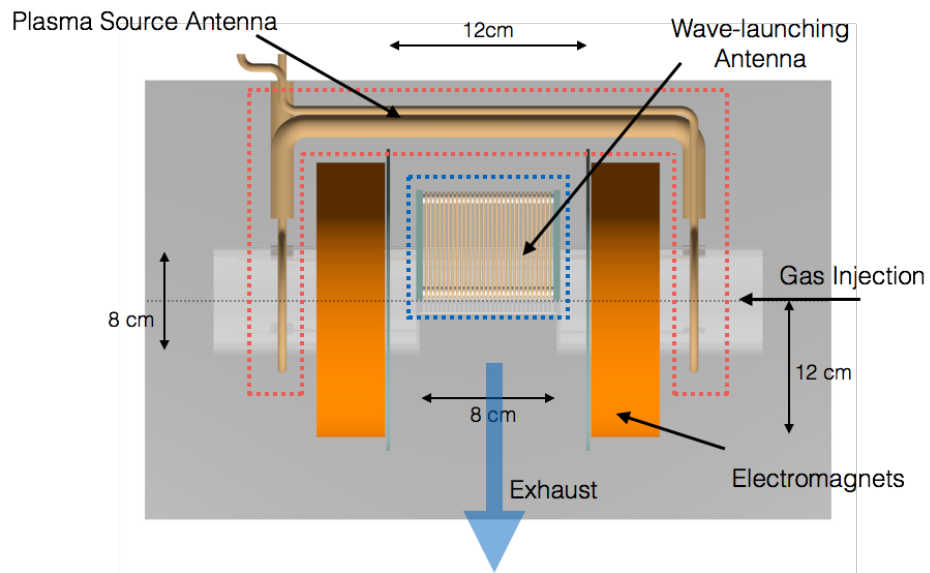


Figure 3. Dimensions for the DWDTX. The confining glass tube has an 8 cm diameter with an 8 cm exhaust hole. The electromagnets have a 12 cm inner spacing and 12 cm outer diameter. The PSA (boxed in red) brackets the two electromagnets. The WLA (boxed in blue) sits directly behind the exhaust hole and is roughly 8 cm x 8 cm.

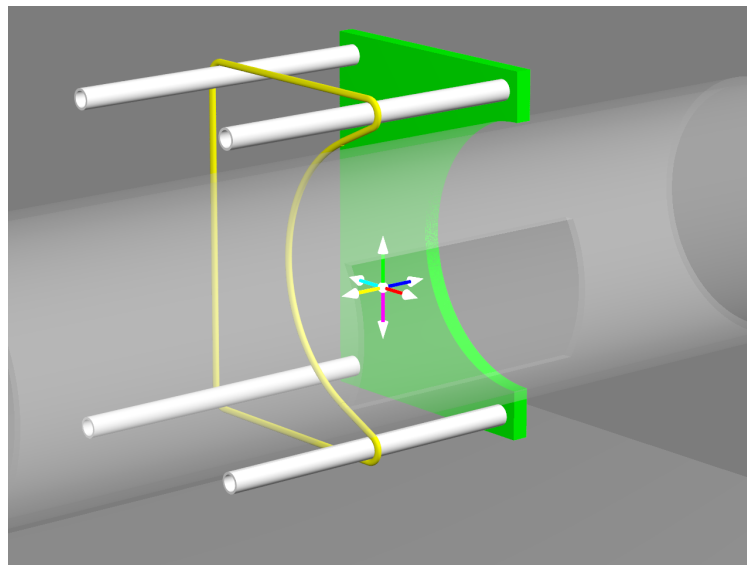


Figure 4. Wave Launching Antenna (WLA). Four alumina rods are mounted between two G10 plates. A single wrapping of the magnet wire is shown in yellow around the alumina rods. The WLA used in this paper has 36 windings over 8 cm.

in Figure 5), the upstream collection area will draw more current than the downstream side. The Mach number and flow velocity can then be determined from^{12, 13}

$$\frac{I_u}{I_d} = e^{kM}, \quad (8)$$

where $I_{u,d}$ are the respective ion saturation currents and k is a calibration constant.

Our probe (shown in Figure 5) consists of two flat copper plates 2 mm in diameter spaced by ceramic insulation .2 mm thick. The probe is designed so that the size of the probe is larger than the Debye length even in the low density plume. Each plate is biased into ion saturation at -27 V and the current is measured over 9.96 kΩ sense resistors.

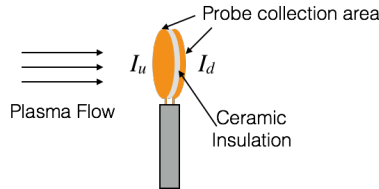


Figure 5. Diagram of DWDTX Mach Probe. Two 2 mm diameter copper plates (1/64" thick) are separated by a 0.2 mm thick ceramic insulator. The probe is positioned so that the plates perpendicularly intersect the plasma flow. Each plate is biased into ion saturation at -27 V and the currents, $I_{sat,u/d}$, are measured across 9.96 kΩ sense resistors.

Significant analytical and experimental work has been performed to determine exact values of k for different probes in both magnetized^{12, 14, 15} and unmagnetized^{13, 16, 17} plasmas. Since our probe is located far from the source, the magnetic field is negligible and the probe should be analyzed using unmagnetized Mach probe theory. For the case of an unmagnetized spherical probe with low ion temperatures, Hutchinson numerically found that $k = 1.34$.¹⁷ Later experimental measurements taken by Oksuz et al. using a Mach probe with a similar plate design to ours found $k \approx 1.3$.^{18, 19} Other models and analysis place k between 1 and 2 when $T_i < T_e$.¹⁵⁻¹⁷ Because of the similarity of our design to the probe used by Oksuz et al., we take k to be 1.3. However, since our probe has not been independently calibrated, our results should be interpreted qualitatively.

C. Data Collection

In order to isolate the effects due to increasing the current and frequency of the WLA, the plasma source was held in a fixed configuration throughout the data collection process. We set the background magnetic field, B_0 , to 30 G and fixed the argon mass flow rate to 2 mg/s. Finally, the PSA power was set to approximately 560 W. This is roughly the same plasma source configuration for which we observed acceleration with the RPA.⁴ At these conditions inside the source, $n_e \approx 2.5 \cdot 10^{17} \text{ m}^{-3}$, and $T_e \approx 5 \text{ eV}$.

For the WLA used, the tuning circuit is capable of accepting frequencies from 200 kHz to 440 kHz. For each frequency tested, power to the WLA was increased to a maximum of 1 kW. Most of this power is lost to the parasitic resistance of the antenna, which increases for increasing frequency.⁴ To make a direct comparison between frequencies, we monitor the current flowing into the antenna via a Pearson current transformer.²⁰ Simultaneously, the MP is used to measure the plasma flow 30 cm downstream from the exit of the source.

Because $T = \dot{m}v_{ex}$ and $M = v/c_s$, ΔM is only proportional to the total momentum transfer when c_s and \dot{m} of the plasma remain constant. We verify that $c_s = \sqrt{T_e/m_{\text{argon}}}$ remains constant by repeating the experiment while taking LP measurements in the exhaust plume. These measurements show the plume temperature to be approximately 7 eV and not change significantly as WLA power varied. However, while the neutral flow of argon to the experiment is kept fixed, we have not yet demonstrated that the mass flow of plasma is constant for increasing power to the WLA, which prevents us from using the Mach probe to make a direct measurement of thrust.

IV. Mach probe results

With no power to the WLA, we measured the Mach number in the plume; $M = 1.50 \pm .02$, and for each frequency, we measured the increase in the Mach number of the plume, ΔM , for increasing rms-antenna current, J_a . This data is shown in Figure 6. For all frequencies tested, we measured an increase in M as J_a is increased. This increase was more substantial at higher frequencies, which qualitatively agrees with both Section II and our previous predictions.³ A maximum ΔM of $0.13 \pm .01$ was achieved at 440 kHz with approximately 500 Ampere-turns of current in the WLA.

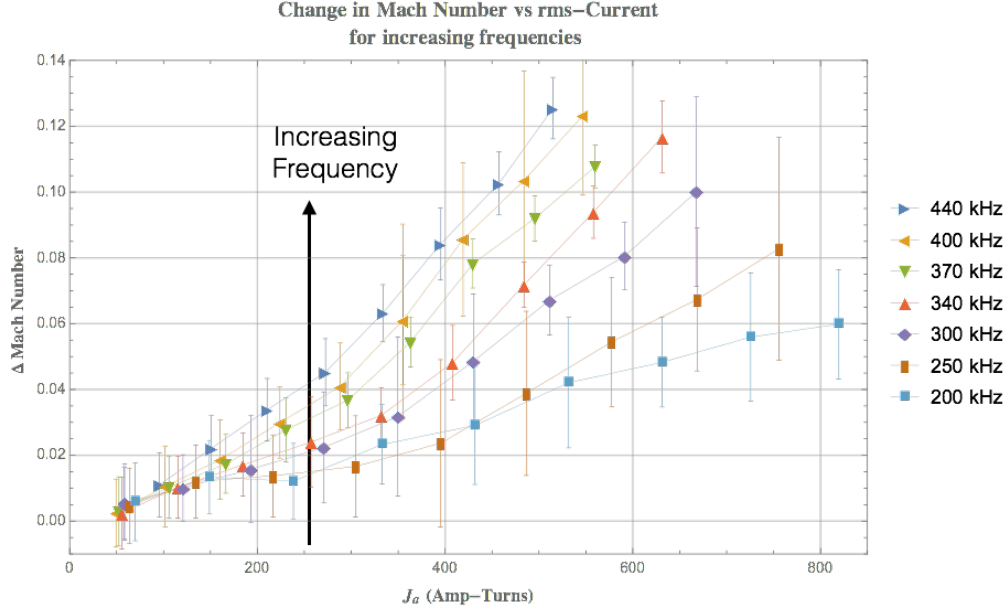


Figure 6. ΔM vs J_a for increasing frequency. The change in Mach number in the plume is plotted against the rms-current in the WLA. The source plasma was generated with $\sim 560\text{W}$, with 2mg/s flow of argon in a $B_0 = 30\text{ G}$ field. Frequency in the WLA was varied from 200 kHz to 440 kHz with increasing frequencies generating larger Mach numbers at high power.

While we cannot use ΔM to make a direct thrust measurement, it is informative to determine the scaling of ΔM against the predicted thrust, $C_T(\omega)J_a^2$, where C_T is calculated for the given experimental parameters and excitation frequencies. This relationship is plotted in Figure 7, and we observe that each data set collapses onto a linear trendline. Assuming that \dot{m} is constant, the observed dependence of ΔM on $C_T J_a^2$ suggests that scaling law described in our model is accurate.

V. Discussion

In this paper, we have derived an analytical approximation for the scaling of momentum transfer in the DWDTX as a function of WLA frequency. This approximation shows that the DWDT thrust coefficient scales as

$$C_T(\omega, n_e, B_0, H, l, d) = \frac{\mu_0}{3\pi} \frac{H^4 l^2 \omega_{pe}^6}{c^6 \Omega_e^3} \left(1 - \frac{3(l+d)H\omega_{pe}^2}{4c^2 \Omega_e} \omega \right) \omega^3. \quad (9)$$

We indirectly validate this scaling law by measuring the change in Mach number, ΔM , of the exhaust plume. Qualitatively, the exhaust Mach number clearly increases for higher applied currents and frequencies. By plotting ΔM against $C_T J_a^2$, the measured data collapses onto a linear trend. However, because we have not validated the assumption of a constant mass flow, we can only indirectly compare our Mach probe data to the analytical theory.

The DWDTX is not optimized, but the derived scaling law suggests that performance can be improved by increasing the size of the system or the density of the source plasma. Improved performance should also be observed for lower magnetic fields. This agrees with our previous RPA measurements, where higher energy ions were observed in the lower magnetic field cases.³ However, decreasing B_0 cannot be done arbitrarily, as

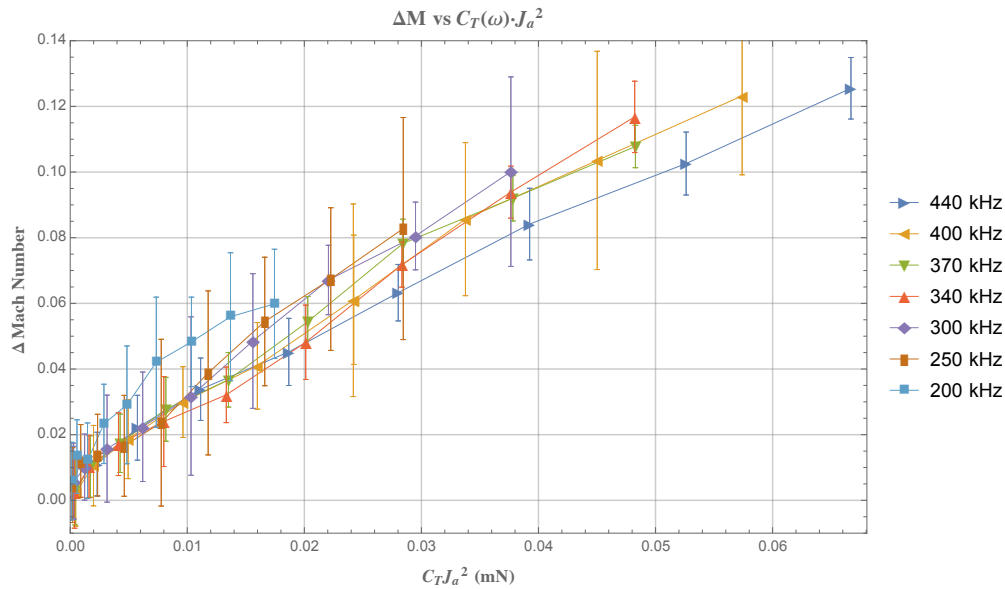


Figure 7. ΔM vs $C_T(\omega)J_a^2$. The change in Mach number is plotted against $C_T J_a^2$ for all frequencies. The data collapses to linear trend line, which agrees with our model's scaling predictions.

the source itself will quickly become unmagnetized. The easiest method for improving momentum transfer is to increase the driving frequency. However, this also cannot be done indefinitely, as the WLA experiences higher resistive losses at higher frequencies. Nevertheless, even in the unoptimized configuration, we measure increases in the exhaust Mach number that follow the our analytical thrust scaling law.

Acknowledgments

The authors would like to acknowledge Bob Sorenson for his invaluable experience with RF power systems as well as the 3d renderings of the experiment. This research was supported by the Program in Plasma Science and Technology (PPST) at Princeton University.

References

- ¹Feldman, M. S. and Choueiri, E. Y., "The Direct Wave-Drive Thruster," *50th AIAA Joint Propulsion Conference*, No. AIAA-2014-4025, Cleveland, OH, July 28-30, 2014.
- ²Jorns, B. and Choueiri, E., "Thruster concept for transverse acceleration by the beating electrostatic wave ponderomotive force," *32nd International Electric Propulsion Conference*, No. IEPC-2011-214, Wiesbaden, Germany, September 11-15, 2011.
- ³Feldman, M. S. and Choueiri, E. Y., "A Direct Wave-Drive Thruster using the Magnetosonic Mode," *34th International Electric Propulsion Conference*, No. IEPC-2015-115, Kobe, Japan, July 6-10, 2015.
- ⁴Feldman, M. S. and Choueiri, E. Y., "Ion Energy Measurements in a Direct Wave-Drive Thruster," *51st AIAA Joint Propulsion Conference*, No. AIAA-2015-3726, Orlando, FL, July 27-29, 2015.
- ⁵Stallard, B., Hooper, E., and Power, J., "Whistler-driven, electron-cyclotron-resonance-heated thruster - Experimental Status," *Journal of Propulsion and Power*, Vol. 12, No. 4, 1996.
- ⁶Diaz, F., "The Vasimr Rocket," *Scientific American*, Vol. 283, November 2000.
- ⁷Pavarin, D., Ferri, F., and et. al., "Design of a 50 W Helicon Plasma Thruster," *31st International Electric Propulsion Conference*, No. IEPC-2009-205, September 2009.
- ⁸Lovberg, R. and Dailey, C., "PIT Mark V Design," No. AIAA-1991-3571, September 1991.
- ⁹Polzin, K. and Choueiri, E., "Faraday Accelerator with Radio-frequency Assisted Discharge (FARAD)," No. AIAA-2004-3940, July 2004.
- ¹⁰Stix, T. H., *Waves in Plasmas*, American Institute of Physics, Springer-Verlag New York, Inc, 1992.
- ¹¹Hutchinson, I., *Principles of Plasma Diagnostics*, Cambridge University Press, 2005.
- ¹²Hutchinson, I., "Ion collection by probes in strong magnetic fields with plasma flow," *Physics Review A*, Vol. 37, No. 11, 1988.
- ¹³Hutchinson, I., "The invalidity of a Mach Probe model," *Physics of Plasmas*, Vol. 9, 2002.
- ¹⁴Stangeby, P., "Measuring plasma drift velocities in tokamak edge plasmas using probes," *Physics of Fluids*, Vol. 27, 2002.

¹⁵Chung, K.-S., Hutchinson, I., LaBombard, B., and Conn, R., "Plasma flow measurements along the presheath of a magnetized plasma," *Physics of Fluids B*, Vol. 1, 1989.

¹⁶Hudis, M. and Lidsky, L., "Directional Langmuir Probe," *Journal of Applied Physics*, Vol. 41, 1970.

¹⁷Hutchinson, I., "Ion collection by a sphere in a flowing plasma: I. Quasineutral," *Plasma Physics and Controlled Fusion*, Vol. 44, 2002.

¹⁸Oksuz, L., Khedr, M. A., and Hershkowitz, N., "Laser induced fluorescence of argon ions in a plasma presheath," *Physics of Plasmas*, Vol. 8, 2001.

¹⁹Oksuz, L. and Hershkowitz, N., "Understanding Mach probes and Langmuir probes in a drifting, unmagnetized, non-uniform plasma," *Plasma Sources Science and Technology*, Vol. 13, No. 2, 2004.

²⁰Pearson Electronics, Inc, *Pearson Current Monitor, Model 411*, 2002.